CHANGE OF PARTICLE ORIENTATION CAUSED BY STATIC SHEARING IN SIMULATED HYDRAULIC FILLED SAND

Ching-Jiang Jeng[1]

ABSTRACT

In this study, the inherent and induced anisotropy of simulated hydraulic-filled specimens determined by microanalyses from thin sections are presented. It is shown that the inherent anisotropy for the orientation of particles of specimens prepared by hydraulic transportation tends to be with the long axis in the horizontal direction, while the result for the wet tamping specimen is quite different. This fabric property is similar to that of in-situ specimens. For the induced anisotropy, the variation of apparent dip angle in vertical direction increases slightly after static shearing. However, even after shearing, the major dip angle of the long axis of particles maintains in horizontal direction. The technique and the methodology employed in this study aid in explaining the mechanical behavior of the hydraulic filled sand.

Key words: Hydraulic filled sand, micro fabric, anisotropy, thin section.

1. INTRODUCTION

For nearly ten years, a series of land reclamation projects using the hydraulic-filled method with flat particle sand has been in progress in middle-western Taiwan. The sand with flat particles is expected to cause by its mother stone which is the sub-metamorphic rock derived from the Central Backbone Range of Taiwan (Wang, 1962). The sand layer is expected to possess inherent fabric anisotropy after filling (Jeng, 1996) which is called inherent anisotropy. Such anisotropy will strongly influence the mechanical behavior (Oda *et al.*, 2001; Vaid and Pillai, 1992; Chung, 1985; Kuerbis, 1985; Shibuya and Hight, 1987). Li and Jeng (1997a) documented that the fabric of hydraulic-filled sand during sedimentation possess inherent anisotropic characteristics. The inherent anisotropy is easily altered in the subsequent shearing process, and new anisotropy (induced anisotropy) is produced. Oda (1997), Oda and Kazama (1998), and Iwashita and Oda (1998) discussed the influence of anisotropy in sand induced by shearing. The results in the previous research indicate that the highly stressed particles are linked in series and that they tend to align like columns whose elongation directions are more or less parallel to the vertical (compression) direction.

Observations were made of the actual micro-phenomenon of fabric change before and after the static shearing for the hydraulic-filled sand. This study applied microanalysis of thin specimen sections that were impregnated with resin. The fabric orientation of the specimens in the initial state and after shearing was observed by microscope. To describe the fabric characteristics of hydraulic filled sand, specimens were prepared using a simulated hydraulic transportation device. Samples prepared by wet tamping (WT) were used for comparison alongside the simulated hydraulic filled (HY) specimens.

The sand used in this study was obtained from the offshore seabed by the Yunlin county in Taiwan. The physical properties

of the sand are summarized in Table 1. Where *a*, *b*, and *c* denote the length of the particle size along the three perpendicular (*i.e.,* long, middle, and short) axes as shown in Fig. 1, respectively. More than hundreds of particles were measured by the results in Table 1. The particle shape of the sand was generally flat. According to the classification of particle shape suggested by Zingg (1935), as shown in Fig. 2, the sand is classified as oblate (disk) (Jeng, 2008). The sphericity of the sand used in this study (*i.e.,* 0.56) is significantly different from other sands (*e.g.* Ottawa sand, Monterey sand, Ticino sand Toyoura sand, *etc.*), typically equal to approximately 0.8 (Been *et al.*, 1987). Photo 1 shows the outward appearance of the test sand under microscope. Figure 3 shows the grain size distribution curve of the sand. The maximum and minimum dry unit weight (γ_{dmax} and γ_{dmin}) shown in Table 1 were obtained using the method suggested by the JIS standard.

The anisotropic characteristics of the specimens, both initial and after shearing, were verified and were considered significant in choosing design parameters and testing methods.

2. TESTING METHOD AND PROCEDURE

The sand used in this study was obtained from the Yunlin offshore industrial park where the land was reclaimed by hydraulic-filling in the sea near mid-western Taiwan.

This study can be divided into four different parts. First, the initial fabric of the HY specimen prepared by sand-water mixture transportation device was observed. Then, an undisturbed thin wall tube specimen, obtained from the field after hydraulic filled construction was used to compare its inherent fabric orientation

[1] Associate Professor, Department of Environmental and Hazards-Resistant Design, Huafan University, Shihding Township, Taipei County 22301, Taiwan, R.O.C. (e-mail: jcjhf@cc.hfu.edu.tw).
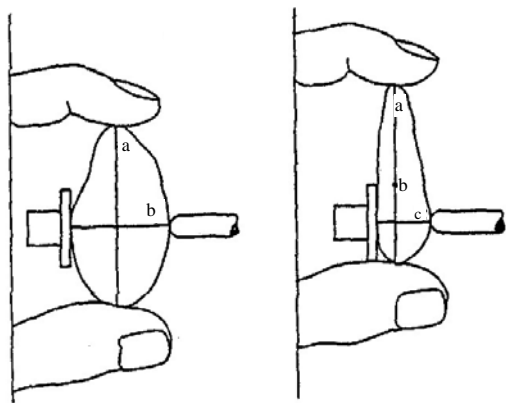
Table 1 Physical properties of testing soils

Classi-fication	γ_{dmax} (kN/cm^3)	γ_{dmin} (kN/cm^3)	Elongation ratio (b/a)	Flatness ratio (c/b)	Sphericity $(bc/a^2)^{1/3}$
SP	15.931	12.518	0.71 ± 0.23	0.42 ± 0.29	0.56 ± 0.19

Fig. 1   The denotation of the long, medium, and short axes of the particles

Fig. 3   Particle size distribution curves

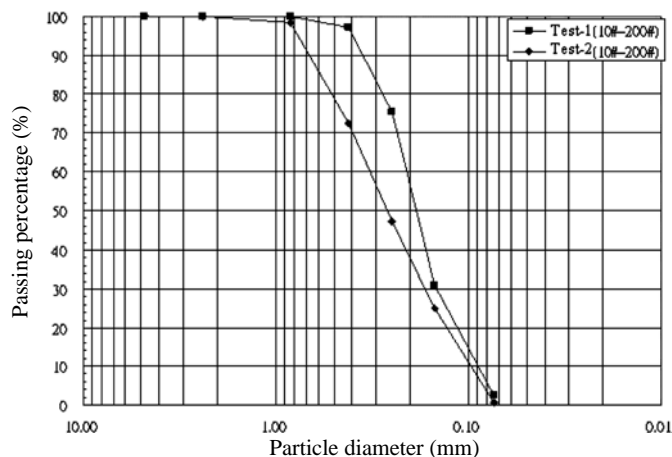**Fig. 2   Classification of particle shape of the testing sand**

Photo 1   Particle shape of testing sand

with the HY specimen. Thirdly, the initial fabric of WT specimen was observed to compare it with the fabric of the HY specimen. Finally, the variation of fabric for the specimen after applying with axial compression and extension were measured. Each step in further details are presented in the following section.

2.1 Simulated Hydraulic Filled Sand Specimen

(1) Testing device and preparing process

The HY specimen was prepared by a sand-water mixture transportation device (Jeng, 1996). Figure 4 shows the detail of the simulated hydraulic sand-water mixture transportation device for preparing the HY specimens. Sand and water were combined with the slurry concentration ($C_w = W_s / W_t$, where W_s and W_t are weights of dry sand and the slurry, respectively) equals about 0.133 in the mixing tank, and then the slurry was pumped into the settling column. Sand particles were freely deposited in this column, while the unsettled slurry flowed back to the mixing tank and circulated again, until the splitting specimen model in the bottom of settling column finished at deposition height. The HY specimen has been proven for its performance in the uniform distribution of particles and density of the tested sample (Li and Jeng, 1997a,b). To verify repeatability of the HY preparation method, Fig. 5 shows the test result curves of stress-strain relationship and excess pore water pressure for two separate specimens prepared in identical conditions.

(2) Resin injection and thin section

The fabric of the specimens in the states of initial and after test was obtained by careful resin injection in the time of above mentioned states and waited for their hardening then cut the solid into thin section. This was accomplished by the following process. During the resin injection, a prepared resin filled in a jar was carefully injected into the specimen from the bottom without disturbance by keeping the surface of the resin jar 1 ~ 2 cm higher than the seepage surface of the specimen. After that, the testing device was set out for about two weeks, then the specimen was cured in an oven at 35°C (Murphy, 1986; Guo, 1994) for about three to five weeks until the specimen hardened. The solid specimen was then cut into sections and polished. The resulting thin sections were 3 × 1.5 cm in length and width with a thickness of about 0.1 to 0.3 mm. The thin sections were then viewed and analyzed under an optical microscope.
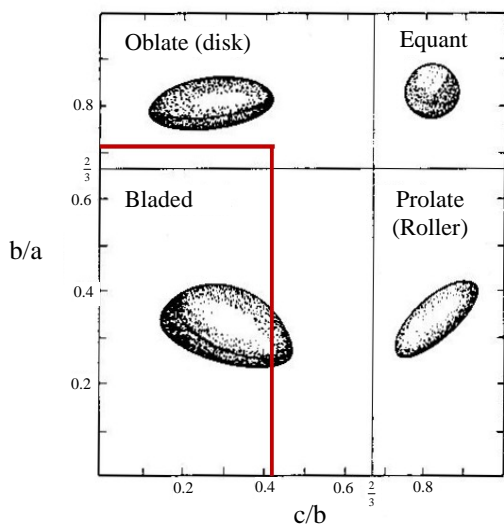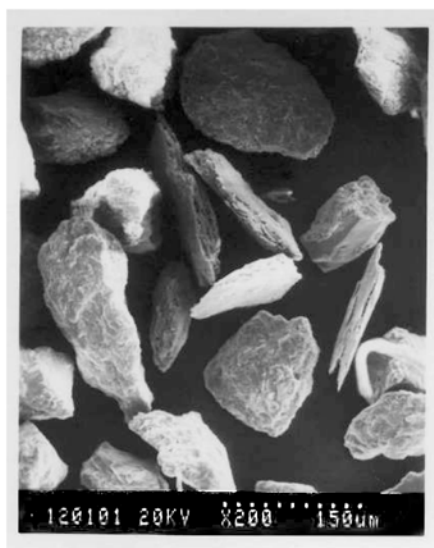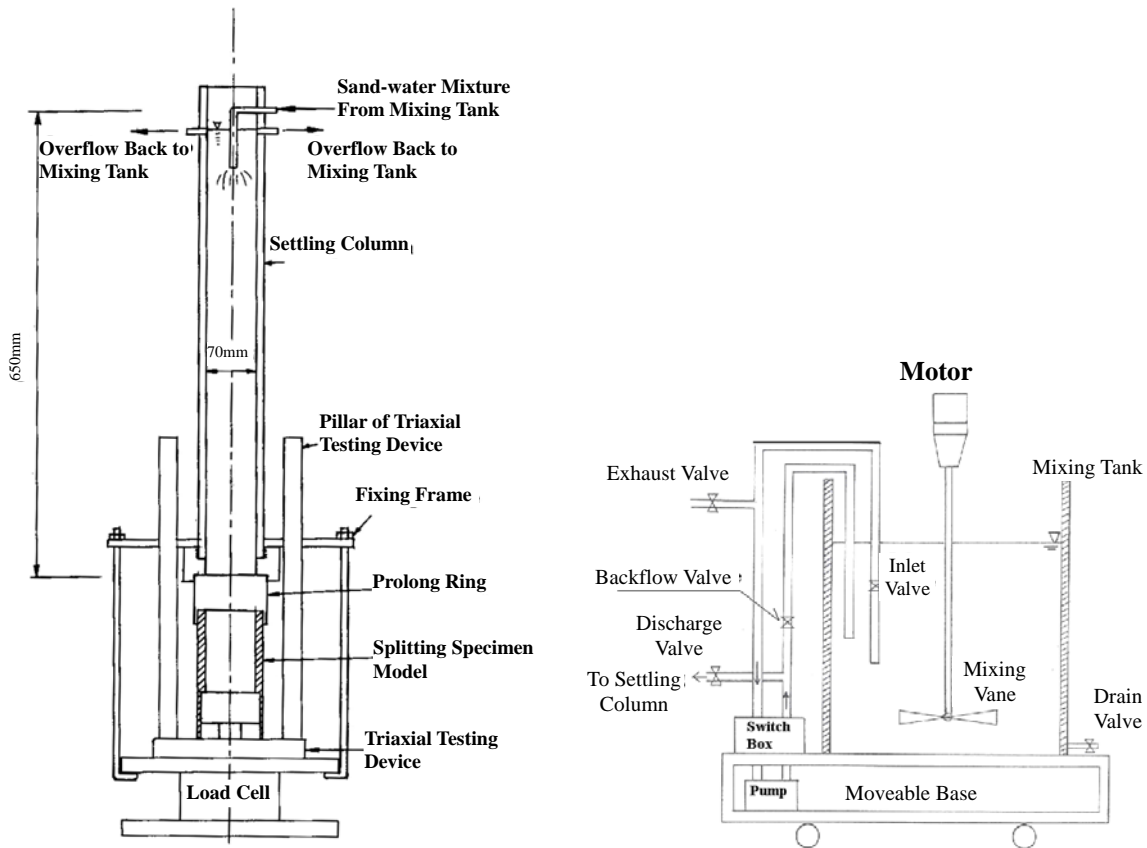
Fig. 4 Sand-water mixture transportation device
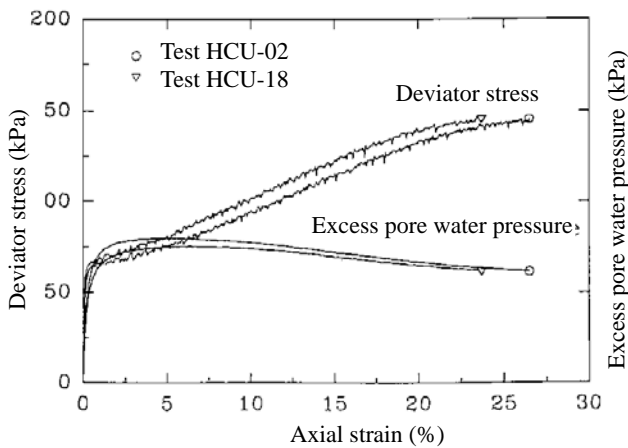

Fig. 5 The repeatability of the HY specimen

2.2 Thin Wall Tube Specimen

The thin wall specimen was taken from the Mai-liao site of the Formosa Plastics Corporation Limited at Yun-Lin County. To minimize the disturbance of the specimen during transportation, storage and cutting, the tube was kept frozen. The procedure of resin impregnation for thin wall tube specimen is similar to that of HY specimens. However, thin wall tube specimen require freezing when cut into small segments and thawing before resin impregnation. To avoid disturbance during the resin impregnation process, the specimen was thawed and then kept at the sur-

face of the resin jar 1 ~ 2 cm higher than the seepage surface of the specimen.

2.3 Wet Tamping Specimen

For comparison, a WT specimen was prepared with 8% water content. It was tamped in a model and was divided equally into six parts. A tamped rod fixed at top for each height accompany with the control volume calculated in advance. When the specimens were made, a slow tamping was performed so that no free drop energy was applied to the specimens, and the fabric of the specimen can be obtained after injection with resin.

2.4 Specimen After Shearing

The HY specimen underwent shearing in undrained conditions with 98 kPa of back water pressure. To maintain its fabric after shearing, resin was injected with pressure equal to the back water pressure.

3. TEST RESULTS

3.1 Fabric of the HY Specimen

The HY specimen was settled in a column and was circulated using a steady slurry of sand-water mixture. Therefore, the sedimentation process was almost symmetric in the horizontal plane. This phenomenon was confirmed by the fabric observations of two orthogonal vertical thin sections. Figure 6 shows the
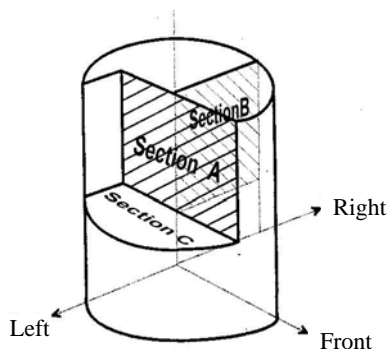
Fig. 6   Schematic diagram of the position of thin sections

Fig. 7   Outline of particles on parts of section A for the HY specimen in the initial state

Fig. 8   The long axis distribution of particles from parts of section A in Fig. 6

direction of the thin section planes. Sections A and B both display similar particle orientations, and their long axes all tend to be in the horizontal direction. On the other hand, the fabric orientation of the horizontal thin section (such as Section C) differs significantly from that of sections A and B. Most of the particles tend to be lying in the plane shape, and few short axes of particles appeared in the horizontal thin section. Figure 7 illustrates the outline of particles observed under the optical microscope on section A for the HY specimen in the initial state, while Fig. 8 shows the distribution of the long axis of the particles from Fig. 7. The rose diagram of the apparent angle of the long axis of particles for the HY specimen can be obtained by measuring the angle between each long axis and the horizontal plane in the counterclockwise direction of the particles and by calculating their percentage corresponding to total particles measured with each 10 degrees of interval. Figure 9 shows the result of the rose diagram for 85 particles. When the particle number was calculated, the initial measurements were taken at an arbitrary location and were sequentially enlarged all sides from particle to particle until all particles of the whole section were measured. Figure 10 illustrates the rose diagram for the area larger than that in Fig. 9. The numbers 5, 10, 15, 20, and 25 as shown in Figs. 9 and 10 denote the percentages of particle long axes. The two rose diagrams illustrate that in the vertical section, the major apparent dip angle of long axes (*i.e.*, the maximum value in rose diagram) was typically about 0 and 180 degree. When defining an occupying percentage in the rose diagram for the area enclosed by the broken line in a variation degree around the major apparent dip angle (*e.g.* the hatches line area in Fig. 10 denotes variation of 10 degree of apparent dip angle) corresponding to the area of the whole rose diagram (*e.g.* the shadow area in Fig. 10), the relationship between the occupying percentage can be obtained for different degrees of variation, and number of particles can be calculated, such as in Fig. 11, which shows that when over 400 particles are calculated, the alteration in value of the occupying percentage is less significant. Thus the calculated result can be meaningful in representation for the fabric.

The curve shown in Fig. 11, indicates that the occupying percentage for 10 degrees of variation based on major apparent dip angle is around 65%. For the curve with 20 degrees of variation, the percentage increases to 86%, while for 30 degrees of variation, the occupying percentage becomes 95%. In other words, the particle tends to orientate in the horizontal direction (0° and 180°) when settled in the HY specimen. The variation of apparent dip angle of particle long axis is approximately 30 degrees.
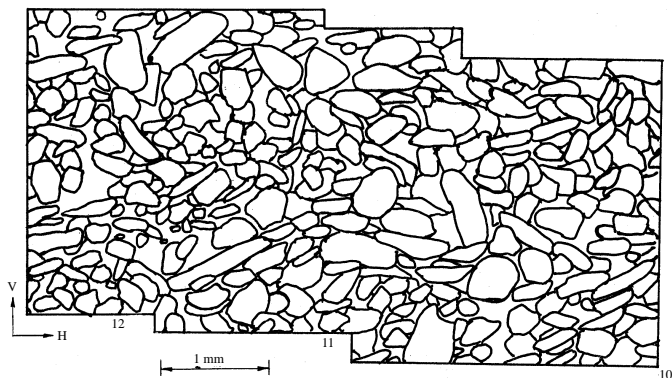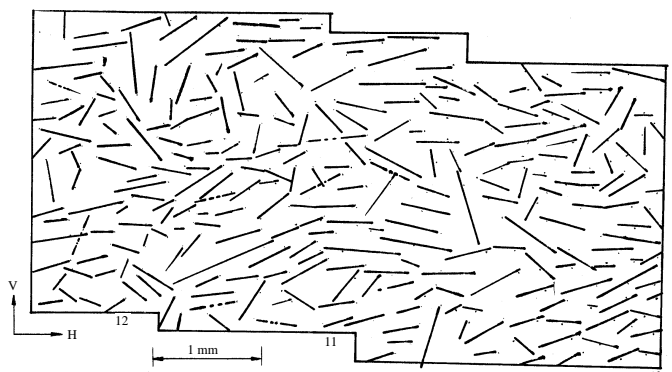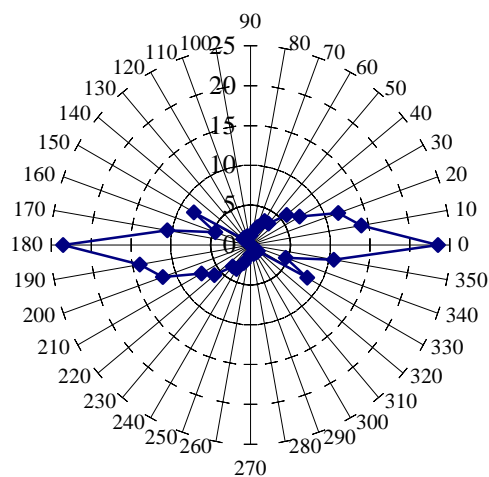

Fig. 9   Rose diagram of the apparent dip angle of the particle long axis on vertical section for the HY specimen (85 particles)

The observation results described above are for the unconsolidated HY specimen. Another specimen was also made to investigate the fabric after traditional isotropic consolidation. The particles orientation was demonstrated not to differ significantly from that of the initial fabric, with the only change being that its void ratio decreased from 1.056 to 1.018 during consolidation.
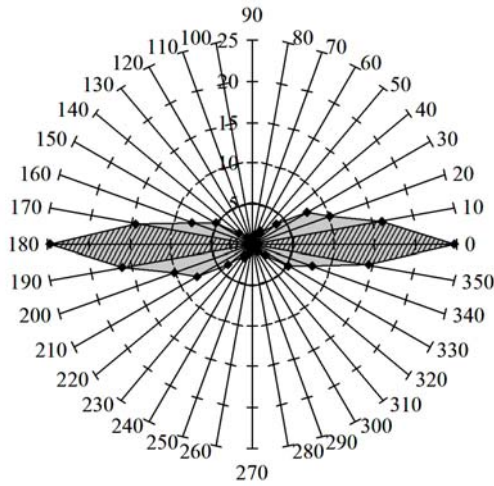
Fig. 10   Rose diagram of the apparent dip angle of the particle long axis on vertical section for the HY specimen (686 particles)
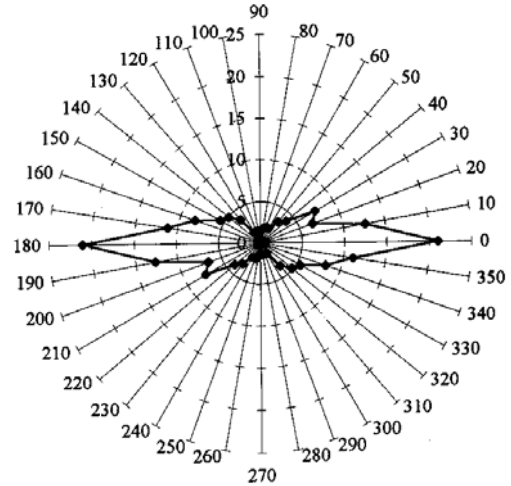

Fig. 12   Rose diagram of the apparent dip angle of the particle long axis on vertical section for the field specimen
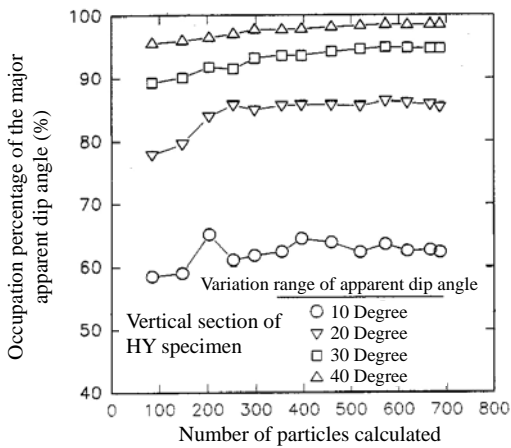

Fig. 11   The relationship between the occupying percentage and number of particles calculated for the HY specimen in initial state
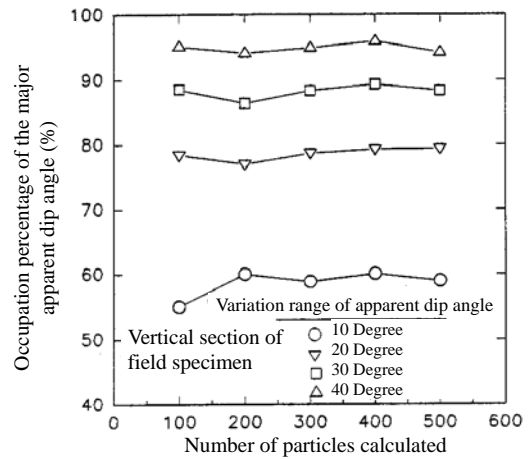

Fig. 13   The relationship between the occupying percentage and number of particles calculated for the field specimen in initia state

3.2 Fabric of the Thin Wall Tube Specimen

Similar fabric can be found in the distributions of long axis of particles and corresponding rose diagram of apparent dip angle for the field specimen, as shown in Fig. 12, which shows the major apparent dip angle to be horizontal (*i.e.*, 0° and 180°). Figure 13 shows the relationship between occupying percentage of particle long axis for different variation and number of particles calculated. It shows that about 60% of long axes range in 10 degrees of variation. If 30 degrees of variation was chosen, about 90% of particle can be enclosed. The analysis result with 30° of variation differ only by 5% with that of HY specimens. For the case with 40° of variation, approximately 4% of difference was illustrated. Figure 14 shows a completely different shape of rose diagram for the horizontal thin section of field specimen. It was learned that the horizontal and vertical sections of HY specimens have significantly different fabric distribution. Accordingly, the anisotropic characteristic of fabric in particles can be clearly observed in the vertical section, while in the horizontal section more isotropic distribution of long axes of particles was illustrated.
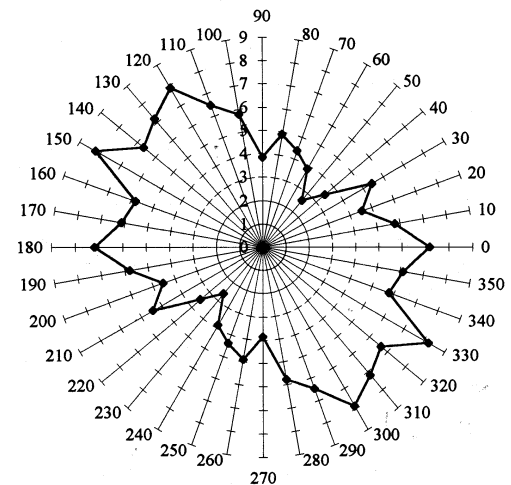

Fig. 14   Rose diagram of the apparent dip angle of the particle long axis on horizontal section for the field specimen (572 particles)

3.3 Fabric of the WT Specimen

A wet temping specimen was used to compare fabric influence owing to different specimen preparation between the simulated hydraulic filled and wet tamping methods. Observations of the vertical and horizontal sections of the WT specimen indicate that the particle orientation is not clearly different between the vertical and horizontal sections. This phenomenon is quite different with the HY specimen. Moreover, the tendency observed in the HY specimens for the long axes of particles to be oriented in the horizontal direction was not observed in the vertical section of the WT specimen. Figure 15 shows the distribution of the long axes of particles of the vertical section for the WT specimen. The figure displays that the particle long axis generally has a random distribution. Figure 16 illustrates the rose diagram for the result of 1355 particles. The tendency for a uniform percentage in each degree of direction increases with the number of particles calculated. When comparing the occupying percentage for major apparent dip angles for 10° of variation, as for the combined result in Fig. 17, the similarity of fabric condition in occupying percentage between the HY specimen and the actual field specimen is clearly better than for the WT specimen. Moreover, the occupying percentage of major apparent dip angle for the HY specimen was around 65%, while that for WT specimens was much less, at about 16% (very near to the ideally homogeneous condition for ten degrees of variation that is approximately 11.1% as shown the dotted line in Fig. 17). Based on these observations, the fabric of WT specimen is generally homogeneous while the inherent fabric of the hydraulic-filled specimen behaves significant anisotropic. This phenomenon verifies that different specimen preparation methods influence fabric.

Figure 17 demonstrates that the fabric orientation of the WT specimen more closely resembles the homogeneous condition. It also shows that when more than 400 particles are included in the calculation, the occupying percentage will approach to a steady value.

3.4 Variation of Fabric for HY Specimen after Shearing

For investigating the fabric change after shearing, HY specimens were sheared in undrained compression and extension tri-axial tests to a nearly steady state condition of excess pore water pressure. Figure 18 shows the axial stress-strain curves and excess pore water pressure of these two tri-axial tests. The liquid type resin was then carefully injected into the specimens without changing their pressure state.

3.5 Fabric of the Specimen under Axial Compression

Figure 19 illustrates the rose diagram of the vertical section for the compressional shearing specimen. The figure reveals that the major apparent dip angle also pointed in the direction of 0° and 180°. However, compared to the rose diagram of the initial condition (*i.e.,* Fig. 10), the percentage of particle long axis in the angle other than 0° and 180° is obvious. The occupying percent of major apparent dip angle, varied from 10° to 40°, is shown in Fig. 20. The state of anisotropy of the initial specimen was decreased by the particles rotation during shearing. Consequently, curve convergence was less evident, such that a larger observation area was needed to clarify its convergence tendency. The fabric of the horizontal section generally had a uniform distribution (Fig. 21) as the initial condition.
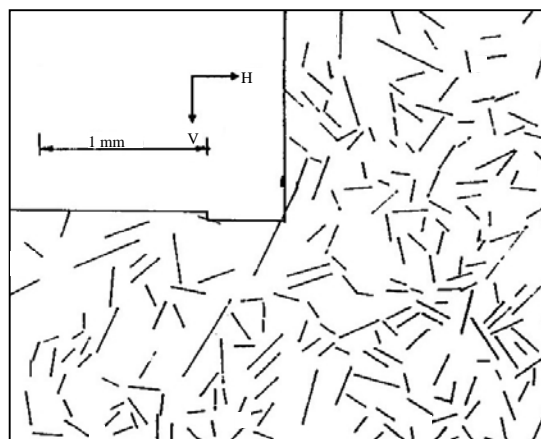

Fig. 15   The distribution of the particle long axis on parts of vertical section for the WT specimen
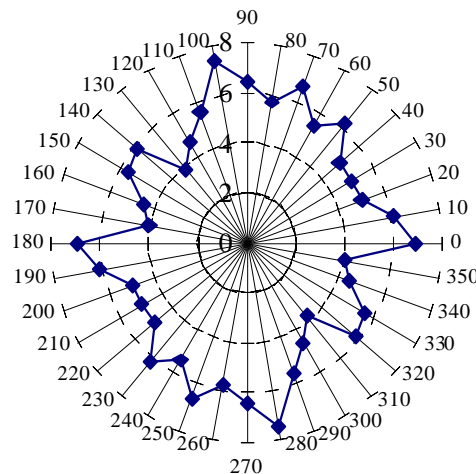

Fig. 16   Rose diagram of the apparent dip angle of the particle long axis on vertical section for the WT specimen (1355 particles)
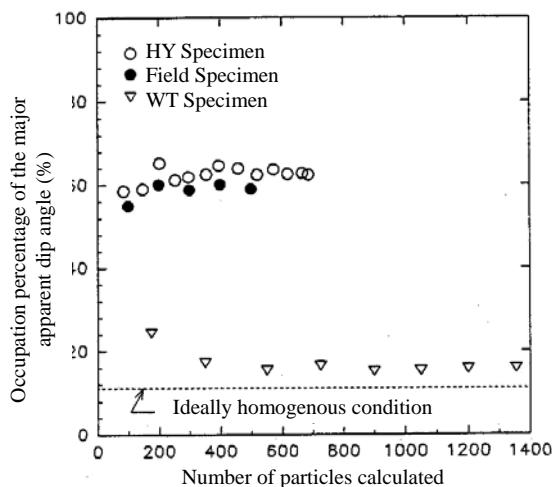

Fig. 17   Comparison on the relationship between the occupying percentage and number of particles calculated for different specimens in initial state with 10° variation
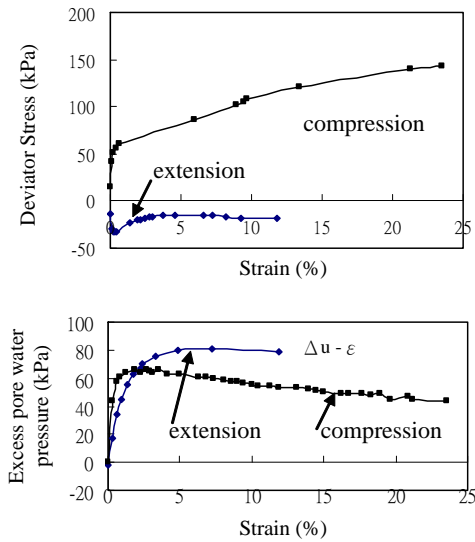
Fig. 18   The stress-strain curves and excess pore water pressure of the HY specimens in axial compression and extension tests
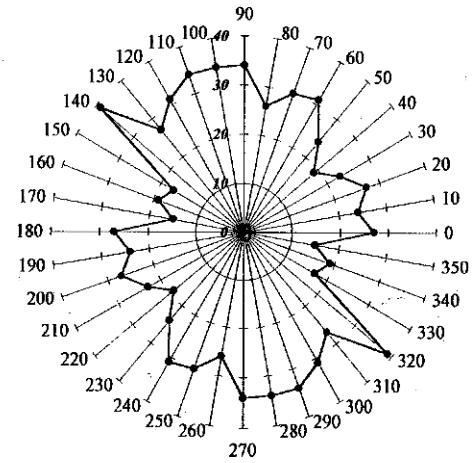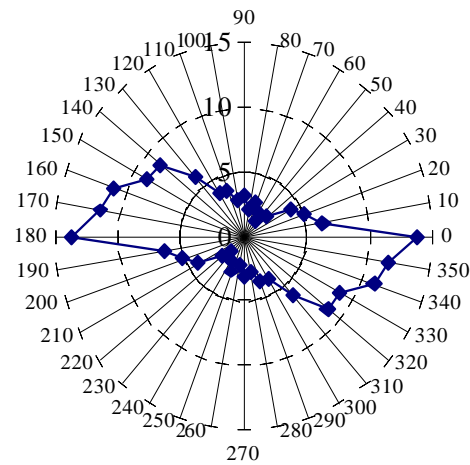

Fig. 19   Rose diagram of the particle long axis on vertical section for the HY specimen after axial compression test (738 particles)

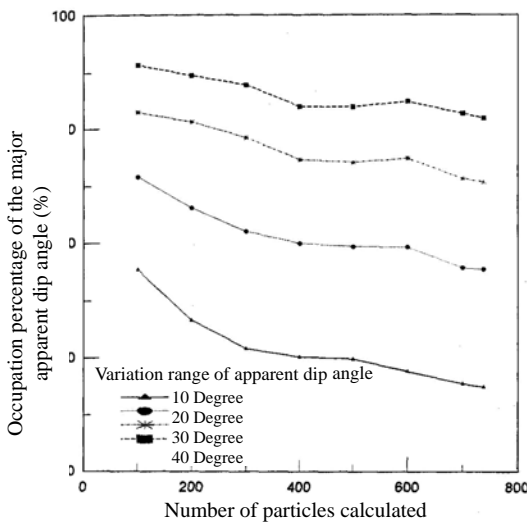**Fig. 20   The relationship between the occupying percentage and number of particles calculated for the HY specimen after shearing**

Fig. 21   Rose diagram of the particle long axis on horizontal section for the HY specimen after axial compression test (481 particles)

3.6 Fabric of the Specimen under Axial Extension

Besides axial compression, an axial extension test was performed and then impregnation with resin, leading to a steady state condition. Figure 22 demonstrates the rose diagram of its apparent dip angle of long axes of particles for vertical section. It can be concluded from the figure that the major apparent dip angle for axial extension testing is also in the horizontal direction (*i.e.*, 0° and 180°). However, the axial value at other angles is relatively larger than that of initial fabric conditions. As for the case of horizontal sections, similar test results with the axial compression condition can be obtained, meaning that the fabric was generally homogeneous in distribution.

3.7 Influence of Stress Path on the Specimen Fabric

The curves in Figs. 20 and 11, indicate that the same variation of apparent dip angle and the percent of the major apparent dip angle before and after the shearing test have several differences. The difference between the actual percentage and 100% is defined as the percentage of divergency. The relationship between divergency and each dip angle variance for different states is compared in Fig. 23; the divergency percentage of the apparent dip angle for the axial extension test is higher than that for the axial compression test. That means the axial extension test results in more fabric change than the axial compression test. However, after shearing, the majority of particle long axes still have a horizontal orientation: this is because the particle rotation is restrained and limited by surrounding particles.

3.8 Phenomenon of Particle Failure Caused by Shearing

In order to find out the breakage caused by particle rotation for the HY specimen after shearing, SEM was used. From the observations, three different kinds of particle failure can be roughly classified. Photos 2 to 4 represent the three types. The first type was caused by compression failure of contact edge marked in photo 2; the second type was caused by bending failure with the particle short axis, photo 3; the third type was
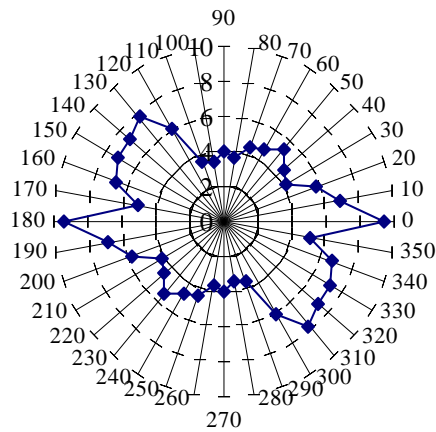
Fig. 22   Rose diagram of the particle long axis on vertical section for the HY specimen after axial extension test (854 particles)
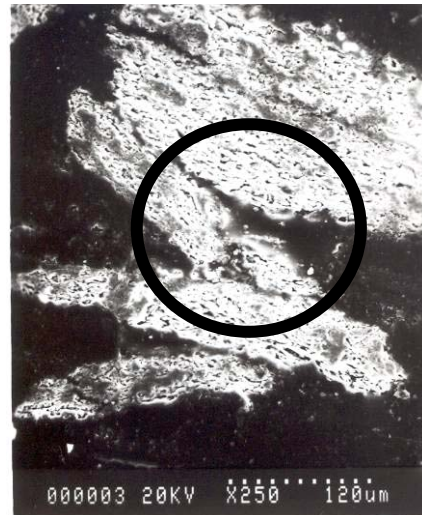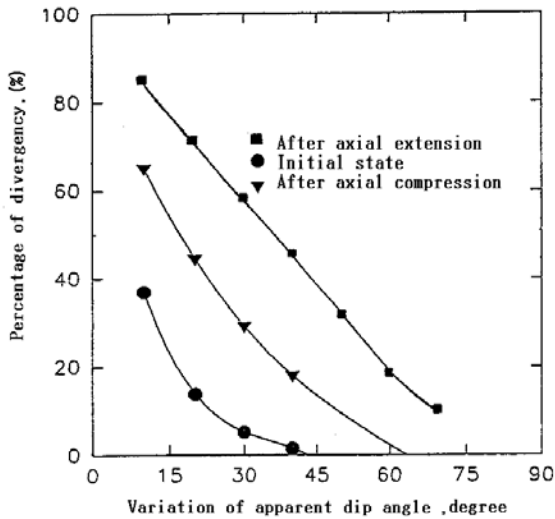

Fig. 23   Comparison on the divergency percentage of apparent dip angle of particle long axis for the HY specimen before and after shearing test

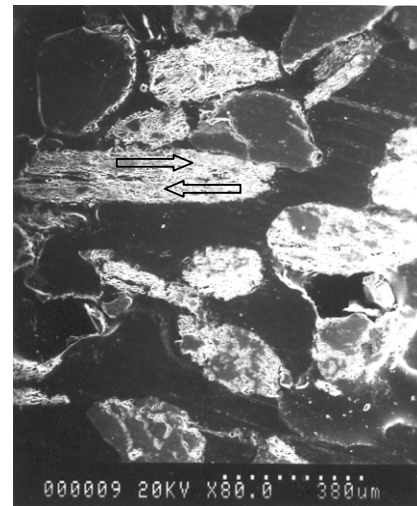**Photo 2   Compression failure of particles**

Photo 3   Bending failure with the particle short axis

Photo 4   Shearing failure along the cleavage of particle
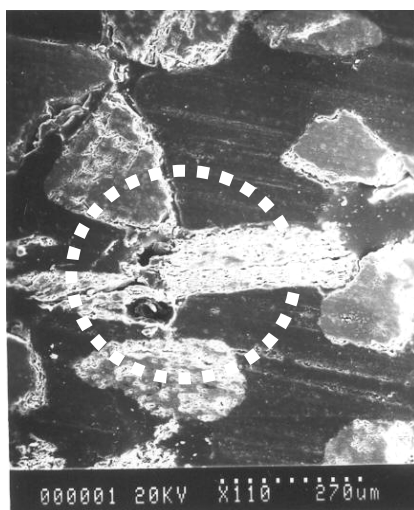
caused by shearing failure along the cleavage of particles, such as the arrow shown in photo 4. Most of the failure observed was classified as the first type. The other two types were less common. That is because most of particle contacts have opportunity to lead to the compression and friction slide between contact points, while for the second and third type of failure, the particle contacts must be arranged in certain specific conditions to cause the particle bending with short axis and shearing failure along the cleavage of particle. Nevertheless, no mater how the particle was orientated, the direction of long axes of particles did not change significantly. Thus after shearing, the major dip direction of long axes tends to be horizontal, the anisotropy of the HY specimen remained even after a considerable shearing deformation had occurred. This observation helps to explain the possible influence of anisotropy on the shearing behavior of HY specimens.

4. CONCLUSIONS

This study examines the fabric of the hydraulic filled specimen using the thin-section method. First, the similarity in fabric of the HY and field specimens was verified. Next, the variation

in fabric was compared both before and after shearing. Observations indicated an obvious inherent anisotropic characteristic in the HY specimen, but no such anisotropy for the WT specimen. The anisotropic characteristic of the HY specimen affects the shearing behavior. Based on the results obtained, the following conclusions can be drawn:

1. The fabric of flat shaped sand specimen prepared by the hydraulic filling method tend to be oriented horizontally. This phenomenon differs from that of the wet tamping specimen.

2. The HY specimen preparation method used in this study can produce a similar fabric to the thin wall tube specimen.

3. The anisotropic fabric of the HY specimen does not disappear completely after intense shearing, due to restraint by surrounding particles, despite the particles being rotated during the shearing process, increasing the divergency of the apparent dip angle of the particle long axis.

4. The shearing characteristic of the flat particle sand is affected by its initial fabric and stress path. Therefore, the amount of particle rotation before and after shearing differs for both axial compression and extension. However, the major apparent dip angle of the long axes of particles remains horizontal in direction.

5. The technique of thin-section used in this study and the methodology discussed provides a way of studying the sand fabric and should be considered in explaining the mechanical behavior of the hydraulic filled sand by the micro- observations conducted.

REFERENCES

Been, K., Jefferies, M. G., Crooks, J. H. A., and Rothenburg, L. (1987). "The cone penetration test in sands: Part (II) general inference of state." *Geotechnique*, **37**(3), 285–299.

Chung, E. K. F. (1985). "Effects of stress path and prestrain history on the undrained monotonic and cyclic loading behavior of saturated sand." Master Thesis, The University of British Columbia, Vancouver, Canada.

Guo, C. H. (1994). "Investigation of sandy soil fabric and particle morphology." Master thesis, Department of Civil Engineering, National Central University, Taiwan (in Chinese).

Iwashita, K. and Oda, M. (1998). "Rolling resistance at contacts in simulation of shear band development by DEM." *J. Engrg. Mech.,* ASCE, **124**(3), 286–292.

Jeng, C. J. (1996). *Shearing Characteristics of the Simulated Hydraulic-Filled Sand with Flat Particles*. Ph.D. Dissertation, Department of Civil Engineering, National Central University, Taiwan (in Chinese).

Jeng, C. J., Li, John C. Liu, S. K., Tseng, C. S., and Chung, Y. H. (2008). "Influence of fabric orientation to the permeability and dynamic characteristics of hydraulic-filled sand." *Soils and Found.,* Tokyo, **48**(2), 221–229.

Kuerbis, R. H. (1985). "The effect of gradation and fines content on the undrained loading response of sand." Master thesis, University of British Columbia.

Li, John C. and Jeng, C. J. (1997a). "Mechanical characteristics of flat shaped hydraulic-filled sand." *Proc. Natl. Sci. Counc. ROC (A)*, **21**(2), 1–12.

Li, John C. and Jeng, C. J. (1997b). "Shearing properties of simulated hydraulic-filled sands with flat particles." *Journal of the Chinese Institute of Civil and Hydraulic Engineering*, **9**(1), 39–48 (in Chinese).

Murphy, C. P. (1986). *Thin Section Preparation of Soils and Sediments*. A B Academic Publishers, Britain.

Oda, M. (1997). "A micro-deformation model for dilatancy of granular materials." *Proc. Symp. on Mech. of Particulate Mat.,* Chang, C. A., Misra, A., Liang, R. Y., and Babic, M., Eds., ASCE, New York, 24–37.

Oda, M. and Kazama, H. (1998). "Microstructure of shear bands and its relation to the mechanism of dilatancy and failure of dense granular soils." *Geotechnique,* London, **48**(4), 465–481.

Oda, M., Kawamoto, K., Suzuki, K., Fujimori, H. and Sato, M. (2001). "Microstructural interpretation on reliquefaction of saturated granular soils under cyclic loading." *Journal of Geotechnical and Geoenvironmental Eng.*, **127**(5), 416–423.

Shibuya, S. and Hight, D. W. (1987). "A bounding surface for granular materials." *Soils and Foundations*, **27**(4), 123–136.

Vaid, Y. P. and Pillai, V. S. (1992). "The critical state of sands: Discussion." *Geotechnique*, **42**(4), 658–660.

Wang, Chao-Siang (1962). "Preliminary investigation on recent sediments of the Chianan coastal plain, western Taiwan." *Memoir of the Geological Society of China*, **1**, 1–10 (in Chinese).

Zingg, T. (1935). *Bietrahe Zur Schotteranalyse*. Schotteranalyse, Mineral Petrography Mitt., **15**, 39–140.